AUTO-ADAPTIVE CONTROL OF A ONE-JOINT ARM DIRECT DRIVEN BY ANTAGONISTIC SHAPE MEMORY ALLOY

D Josephine Selvarani Ruth, S Sunjai Nakshatharan and K Dhanalakshmi
Department of Instrumentation and Control Engineering
National Institute of Technology, Tiruchirappalli, India
E-mail: djsruth@gmail.com, sunjainakshatharan@gmail.com, dhanlak@nitt.edu

Submitted: Apr. 12, 2013 ***Accepted: May 2, 2013*** ***Published: June 5, 2013***

Abstract— This paper pursues a promising approach to obtain strain feedback based angular motion control of a manipulator for any robotic application. The proposed single degree of freedom manipulator uses antagonistic shape memory alloy (SMA) actuated wires. Antagonistic SMA actuated structures employ opposing pairs of one-way SMA actuators to create systems capable of a fully reversible response. A self-tuning PID type fuzzy (auto adaptive) based control scheme is designed and implemented experimentally. The controller is designed based on the model estimated by using system identification technique. Experimental and simulation results show that antagonistic SMA actuator in combination with the controller can track any input trajectory signal with high accuracy motion control and is suitable for various control applications.

Index terms: Shape Memory Alloy, Antagonistic Angular Motion Control, One-Joint Arm Manipulator, Self-tuning Fuzzy PID

I. INTRODUCTION

Shape memory alloy (SMA) exhibit unique remarkable properties such as high force to weight ratio, high strain capability, corrosion resistance, light weight, large electrical resistivity, good ductility and long fatigue life. These inherent properties have enabled SMA to be used as actuator. To meet the demanding applications of miniature robotic manipulations, many unconventional actuators have been developed. They include thermal [1-2], pneumatic [3], ionic polymer metal composite [4], piezoelectric [5], magnetic [6] and SMA [7-12] actuators. SMA can be electrically activated; thereby as an actuator it replaces motors and solenoids. It provides potentially simple, silent and smooth operation and auto sensing (self-sensing) ability. SMA as a linear element (a wire) determines its pre-determined shape when transformed from a pre stretched low temperature martensite state to a higher temperature austenite state by which it provides controlled action that can be utilized to generate mechanical work. For repetitive and desired actuation, the SMA element needs to be properly biased at the end of each heating-cooling actuation cycle. One type of configuration is a bias type actuator that uses SMA along with a bias element (spring). Another type is to use two SMA wires connected antagonistically in which one wire is heated while the other is cooled. In the former there is no active control of movement when the SMA is naturally cooled. Hence better controllability and response can be obtained from antagonistic configuration in comparison with the bias spring configuration. Tracking control is indispensable in many applications such as vibration control, robotic applications and so on. As a result of hysteresis, an inherent nonlinear behavior is associated with SMAs and that's why tracking control of SMA actuators has become an interesting task. Variety of models has been developed for SMA actuators. Literature review finds the use of SMA actuators for tracking control system using the model of Brinson et al. in [13]. SMA actuators for position control system using self-tuning fuzzy PID controller for a single SMA wire is reported in [14]. Lately, Tabrizi et al. have presented a nonlinear position control of antagonistic shape memory alloy actuators which uses a constitutive model, phase transformation model and a heat transfer model [15]. This work is from the motivation in the use of low degree-of-freedom robots to perform intricate manipulation, the academic interest to understand the simplest mechanisms capable of performing a given mission and the economic motive to build simpler and cheaper robots. Simple robots employing dynamic non-prehensile manipulation may be especially effective in industrial parts feeding or in space, where dynamic effects dominate. To demonstrate this, the design and implementation of self-tuning fuzzy PID control of antagonistically connected

SMA as trajectory tracking actuator for servo control of any robotic manipulator is experimented. This angular motion control is carried out by tuning the parameters of the PID controller, which can then be used to improve the inference and implement a fuzzy adaptive PID controller, which can be used to improve the control performance of system. Further the controller performance is evaluated on an experimental system. The one joint arm manipulator is controlled through MATLAB Simulink package program via a data acquisition system.

II. ACTUATOR DESIGN

The work generation potential of antagonistic shape memory actuators is determined by specific SMA element characteristics and their assembly conditions. In this work two SMA wires are connected in antagonism to apply forces to a pulley alternatively, in opposite direction in order to track any input signal [6] as shown in Figure 1. Based on this literature, each SMA follows the stress-strain relationships given by equations (1) and (2)

$$\dot{\sigma}1 = \frac{\Omega\varepsilon_{1T}\left(T_{1,}\sigma1\right) + \theta_t}{1 - \Omega\varepsilon_1\left(T_{1,}\sigma1\right)}\alpha_1 i_1^2 + \frac{D}{1 - \Omega\varepsilon_1\left(T_{1,}\sigma1\right)}\dot{\varepsilon}_1 \quad - \frac{\Omega\varepsilon_1\left(T_{1,}\sigma1\right) + \theta_t}{1 - \Omega\varepsilon_1\left(T_{1,}\sigma1\right)}\beta_1(T_1 - T_a) \qquad (1)$$

$$\dot{\sigma}2 = \frac{\Omega\varepsilon_{2T}\left(T_{2,}\sigma2\right) + \theta_t}{1 - \Omega\varepsilon_2\left(T_{2,}\sigma2\right)}\alpha_2 i_2^2 + \frac{D}{1 - \Omega\varepsilon_2\left(T_{2,}\sigma2\right)}\dot{\varepsilon}_2 - \frac{\Omega\varepsilon_2\left(T_{2,}\sigma2\right) + \theta_t}{1 - \Omega\varepsilon_2\left(T_{2,}\sigma2\right)}\beta_2(T_2 - T_a) \qquad (2)$$

In antagonistic configuration, the strain (ε) produced by SMA 1 and 2 are related as

$$\dot{\varepsilon}_1 \quad = -\dot{\varepsilon}_2 \qquad (3)$$

The resultant torque *T* applied by the SMA wires is given by

$$T = (f_1 - f_2)r = (\sigma_1 - \sigma_2)Ar \qquad (4)$$

where f_1 and f_2 are the forces generated by SMA1 and SMA2 respectively, '*A*' is the cross sectional area of the SMA wires and '*r*' is the radius of the pulley to which the actuator wires are connected. The radius of the pulley and the length of the SMA wire decide the angle of rotation and strain and torque acting on the pulley respectively. From design aspect a relation is established between the angle of deflection θ of the centrally hinged one-joint arm to the strain of the SMA wire from Figure 2.

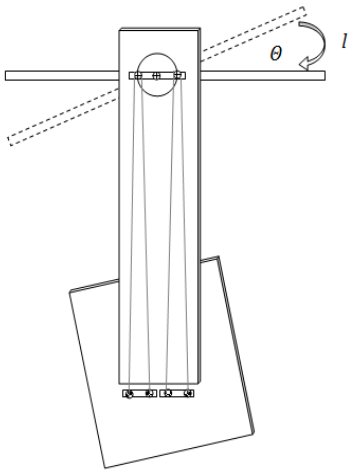

Figure 1. Antagonistic actuation

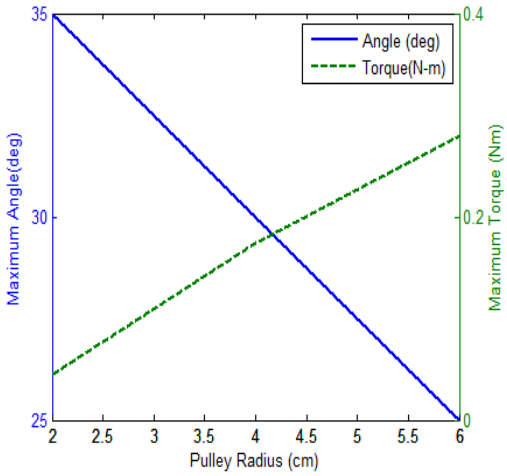

Figure 2. Torque and angle in relation with pulley radius

The radius of the pulley and the length of the SMA wire decide the angle of rotation and strain respectively. For 4% strain of the SMA wire (according to the manufacturer's data), it offers a strain of 1.6 cm for the length of 40 cm of the wire used in the arrangement.

A relation is established between the angle of deflection (θ) of the arm to the arc length (l) produced by the SMA wire.

$$\frac{2\Pi r\theta}{360^\circ} = l \tag{5}$$

$$T = (\sigma 1 - \sigma 2) A \frac{\varepsilon}{2 \sin\frac{\theta}{2}} \tag{6}$$

$$T = (\sigma 1 - \sigma 2) A \frac{l}{\theta} \tag{7}$$

where l is the length of the arc which is related to the strain of the wire by $l = \frac{\varepsilon\theta}{2 \sin\frac{\theta}{2}}$. Hence for any application, the angle of rotation depends on the length of the SMA actuators and the radius of the pulley. The system is designed based on the above relations. For different radius (2cm, 4cm, 6cm) the variation in the angular displacement and the torque produced are shown in Figure 2. Lesser the radius (2 cm) it produces more angles while it introduces heating and cooling delays and creates lesser torque for the beam to track. Higher the pulley radius (6cm) creates lesser angular displacement and creates higher torque. The optimum radius for this beam system is found to be 4cm pulley radius. Hence for any application, the angle of rotation depends on the length of the SMA actuators and the radius of the pulley.

III. SYSTEM DESIGN AND CONTROL

A. Experimental arrangement of the system

To test the manipulation capability of a single joint, a one joint direct-drive robot arm is constructed to perform experiments in dynamic manipulation in Figure3. A horizontal beam of length 60 cm is centrally hinged to a vertical structure at a height of 50 cm which plays the role of a robotic arm. The arm (beam) rotates around a common shaft to one side end of which a pulley of radius 4 cm is fixed. The structure houses two SMA wires attached to the pulley along its diameter to provide antagonistic actuation. Each SMA wire is connected to be mechanically in parallel but electrically in series. Such a configuration offers double the strain and force, in addition provides ease of connection. The specifications of the NiTiNOL SMA (flexinol®) are shown in Table 1. The SMA wire dimensions are designed for optimum force balance and angle of rotation from -30 to +30 degree.

The angular position of the beam is sensed from (5.5 V - 8.5V) by a wire wound rotary 10 K potentiometer connected to the shaft of the beam. This resistance signal is fed back to the controller through the USB 1408 FS data acquisition card with a 14 bit resolution.

B. Control Schematics

A schematic of the experimental design is shown in Figure 3. To track the input signal a PID based control scheme is designed and implemented in Matlab/Simulink which is interfaced with the hardware. A multi-function data acquisition card is employed to acquire the change in resistance (sensor signal) of the actuator via the input port and send the control signal to the SMA actuators via two analog output ports and amplifier circuits (OPA547)/voltage to current converters.

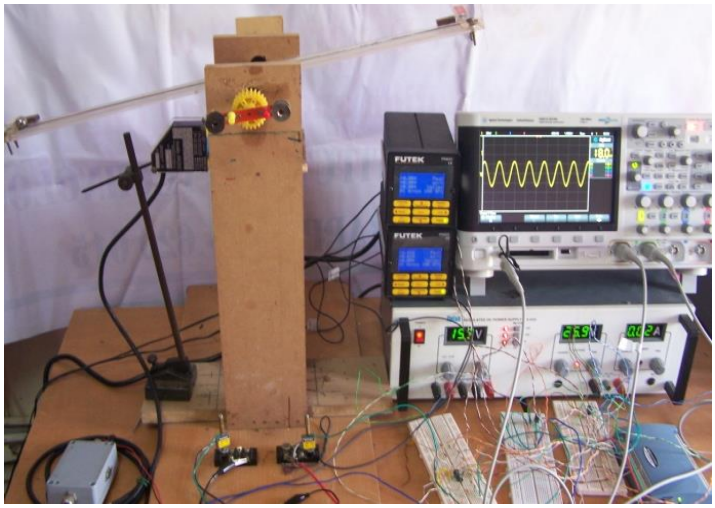

Figure 3(a). Photograph of experimental setup

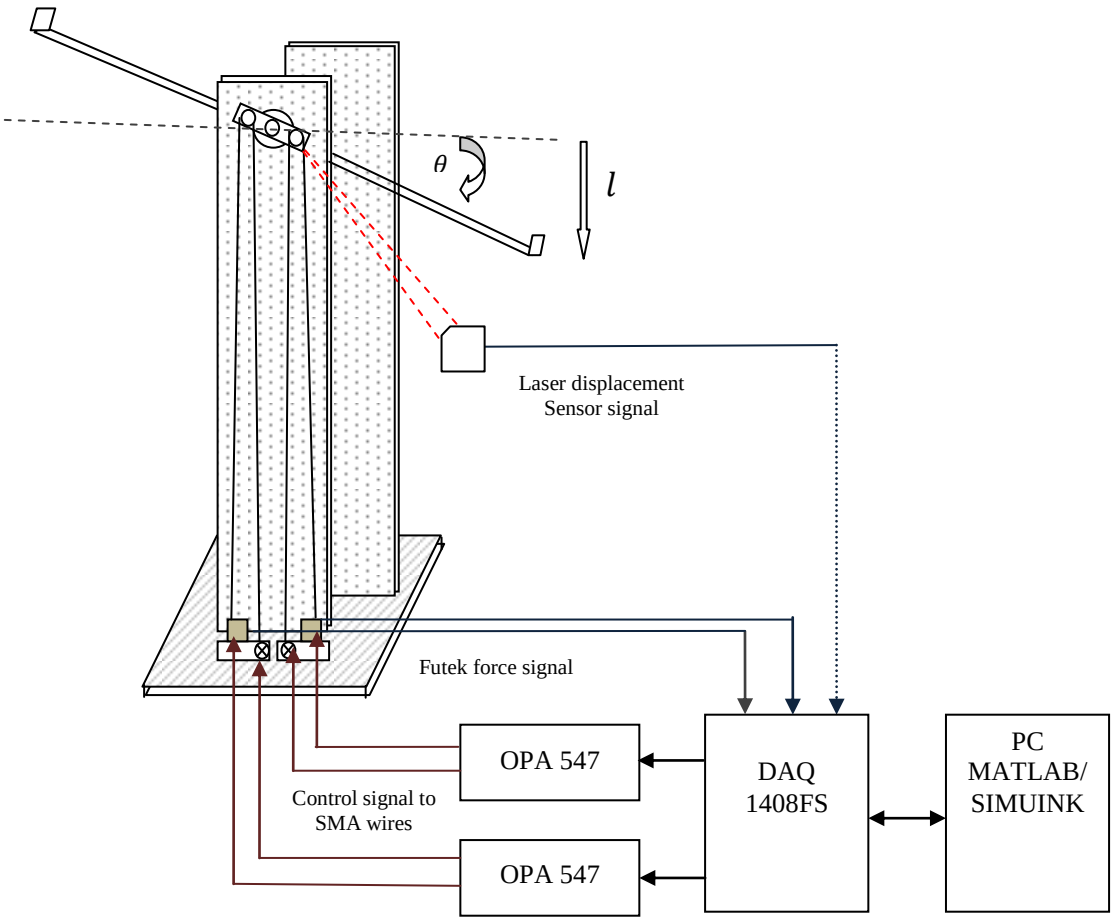

Figure 3(b). Schematic diagram of the hardware

Table 1: Dimensions and properties of the SMA wire

Length (cm)	80
Diameter (cm)	0.01
Transition Temperature (^{o}C)	90
Martensite Start Temperature (^{o}C) Martensite Finish Temperature (^{o}C) Austenite Start Temperature (^{o}C) Austenite Finish Temperature (^{o}C)	72 62 88 98
Hysteresis (^{o}C)	20
Young's modulus Martensite (GPa) Young's modulus Austenite (GPa)	28 75
Density (kg/m^{3})	6450
Resistance (ohm/m)	126
Approximate Current at room temperature (A)	0.200
Maximum Pull Force (kg)	0.143

The OPA547 is internally protected against over-temperature and current overloads. In addition, the OPA547 is designed to provide an accurate, user-selected current limit. Unlike other designs which use a “power” resistor in series with the output current path, the OPA547 senses the load indirectly. This allows the current limit to be adjusted from 0 mA to 750 mA with a 0 μA to 150 μA control signal. This is easily done with a voltage-out or current-out DAC. These circuits provide current to the antagonistic SMA actuators to track the input signal and attain angular tracking of the one joint arm.

IV. MODELING AND CONTROL OF THE ACTUATOR

A. Model identification

In order to obtain the most accurate dynamics of one joint arm SMA actuated manipulator modeling via system identification approach is implemented. System identification based on experimental approaches faithfully represents the dynamic characteristics of the system incorporated with smart materials, and avoid the tangled mathematic or physical models. It deals with the problem of building mathematical models of dynamical systems based on observed data from the system. Identification of parametric model involves selection of model structure, a numerical method for computing a model estimate and model validation. In practice, significant idea about the required plant dynamics and type of structure will assist in selecting the model structure. The prediction error estimate method based on state space model is selected for linear system identification as its estimation accuracy is good comparable with other similar methods. The input and output signals are as shown in Figure4. In order to estimate the system model, the data is divided into two parts; the first part to determine the model and the second part is applied to validate the model.

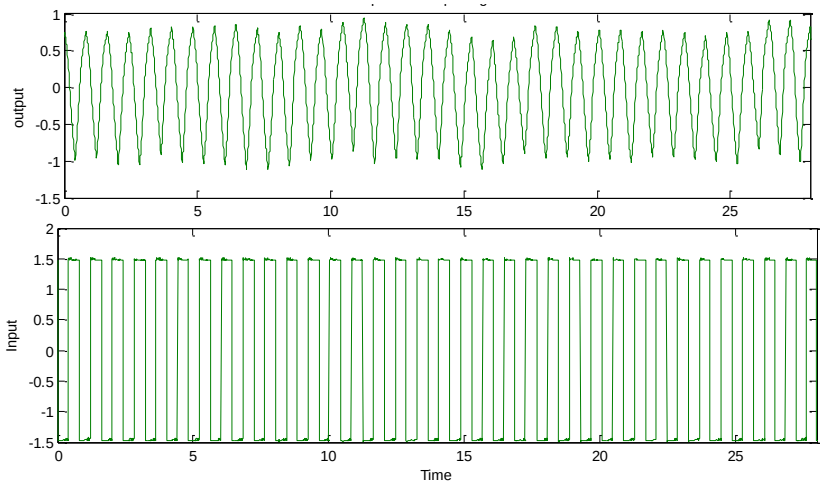

Figure 4. Input and output signals

Figure 5 depicts the validation curve for a second order transfer function between the output and control input for the SMA actuated manipulator in continuous form as given by eq. (8),

$$G(s) = \frac{1.5846s + 42.7412}{s^2 + 13.5807s + 50.3630} \tag{8}$$

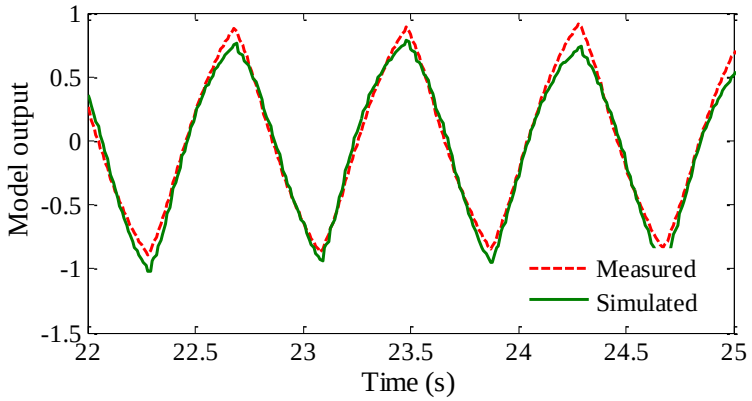

Figure 5. Measured and simulated model output

Here the loss function = 0.00025704and Final Prediction Error (FPE) = 0.00026552. The fit percentage is found to be 90.4%. Increasing the order does not improve the fit percentage, so the lowest order model with best fit is selected. The best model will have all its poles and zeros within the unit circle to show the stability as for this system seen in Figure 6.

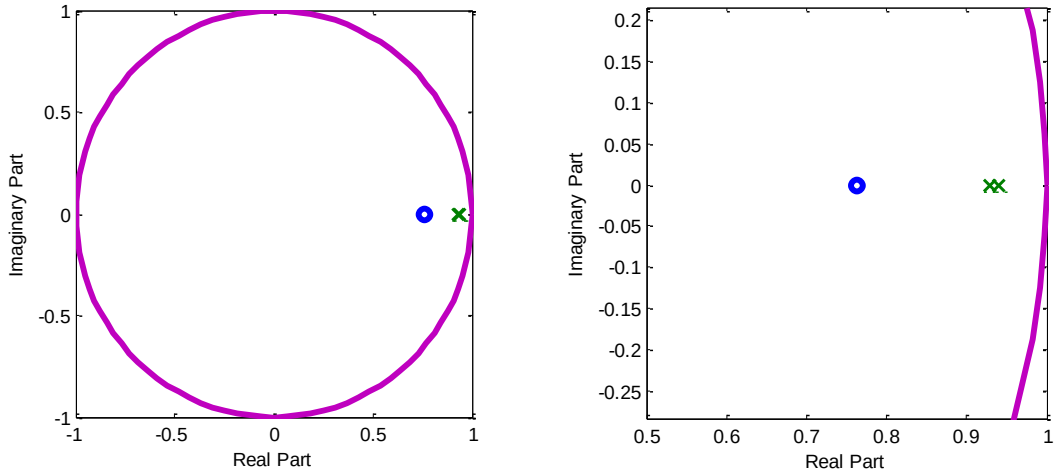

Figure 6. Pole and Zero for the model

The plot in the Figure shows that all poles and zeros are within the unit circle. This is called a minimum phase model; this model address the rule of causality and stability and it would be used for further analysis. From this, analysis on the transient response and frequency response are done and shown in Figure 7 and Figure 8 respectively.

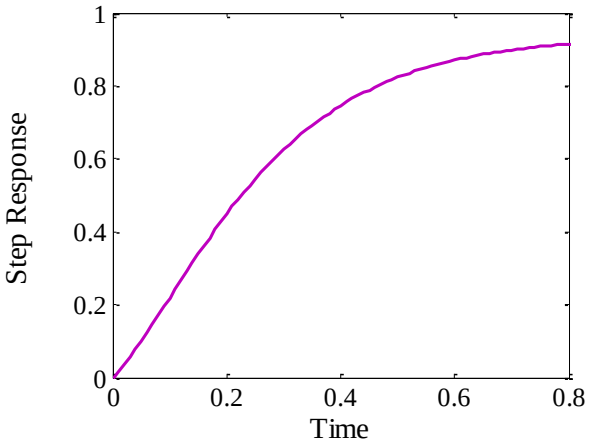

Figure 7. Transient response of the model

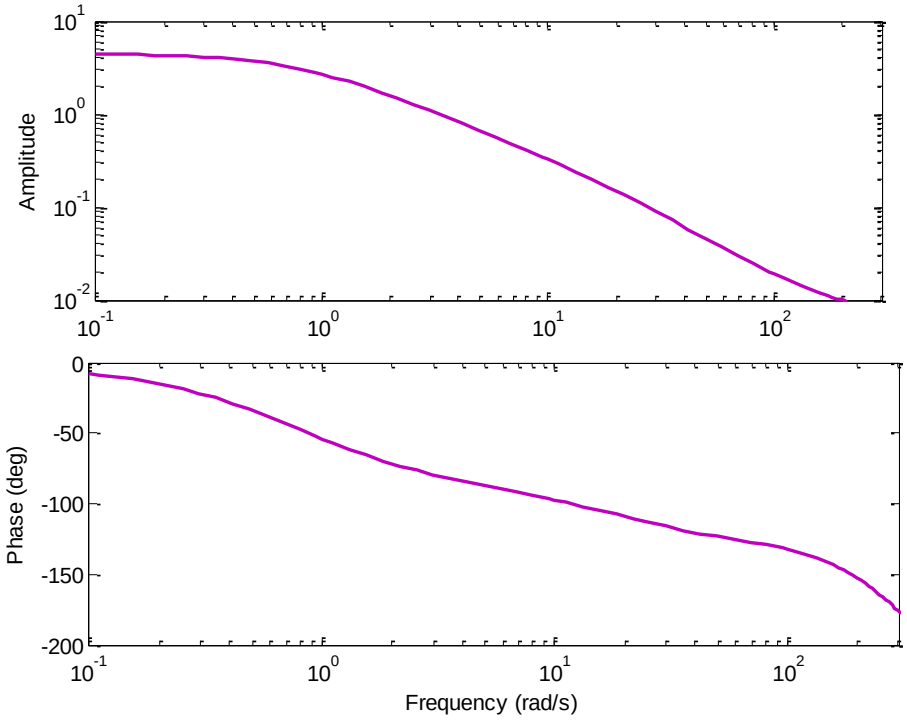

Figure 8. Frequency response of the model

V. CONTROLLER DESIGN AND VALIDATION

The self-tuning PID-type fuzzy controller is an auto adaptive controller that is designed by using an incremental fuzzy logic controller in place of the proportional term in the conventional PID controller to tune the parameters of PID controller on line by fuzzy control rules. The controller uses the error and the rate of change of error as its inputs and to meet the desired self-tuning parameters based on time-varying e and $\dot{e}$.

$$y(t) = Kp\, e(t) + Kd\frac{de(t)}{d(t)} + Ki\int_0^t e(t).d(t) \tag{9}$$

where $K_i = K_p/T_i$ and $K_d = K_pT_d,T_i$ is integral time parameter, T_d is derivative time parameter equation (9). Because the proposed fuzzy self-tuning PID controller aims to improve the control performance yielded by a PID controller, it keeps the simple structure of the PID controller and it is not necessary to modify any hardware parts of the original control system for implementation. Fuzzy self-tuning of PID parameters is finding out the fuzzy relation between the three PID parameters K_p, K_i and K_d. It examines continuously e and $\dot{e}$ then tunes the three parameters with fuzzy control rules online so that the controlled objects achieve better dynamic steady performance.The structure of the self-tuning fuzzy PID controller is shown in Figure 9 where e is the error between actual position and set point and the output, $\dot{e}$is the derivation of error. The PID parameters are tuned by using fuzzy inference, which provide a nonlinear mapping from the error and derivation of error to PID parameters.

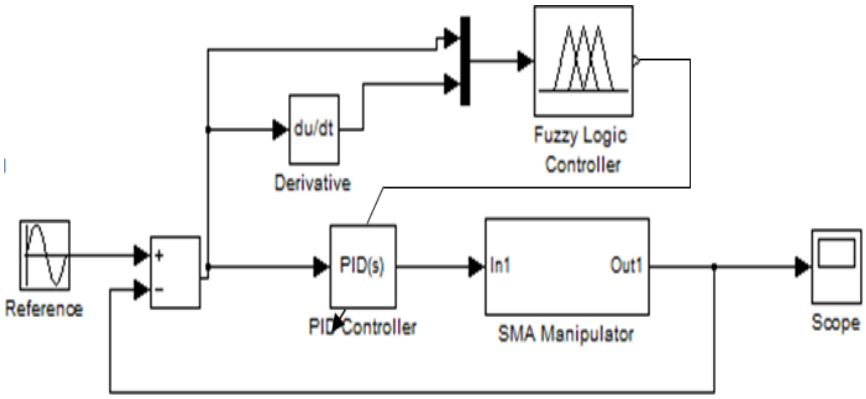

Figure 9. Controller structure

The fuzzy rules designed are based on the characteristic of the antagonistic shape memory alloy actuator and properties of the PID controller. Therefore, the fuzzy reasoning of fuzzy sets of outputs is gained by aggregation operation of fuzzy sets inputs and the designed fuzzy rules. The aggregation and defuzzification method used are respectively max-min and centroid method. Regarding the fuzzy structure, there are two inputs to fuzzy inference: error $e(t)$ and derivative of error $de(t)$, and three outputs for each PID controller parameters respectively K'_p, K'_i and K'_d. Mamdani model is applied as structure of fuzzy inference with some modification to obtain the best value for K_p, K_i and K_d. Fuzzy inference block of the controller design is shown in Figure 10.

The variable ranges of the parameters K_p, K_i and K_d of PID controller are respectively $[K_{pmin}, K_{pmax}]$, $[K_{imin}, K_{imax}]$ and $[K_{dmin}, K_{dmax}]$. The range of each parameter was determined based on the simulation on PID controller to obtain feasible rule bases with high inference efficiency. The range of each parameter are K_p= [1,80], K_i =[0,1] and K_d=[0,0.1]. Therefore, they can be calibrated over the interval [0, 1] as follows:

$$K'_p = \frac{K_p - K_{pmin}}{K_{pmax-K_{pmin}}} = \frac{K_p - 1}{80 - 1} \qquad 10(a)$$

$$K'_i = \frac{K_i - K_{imin}}{K_{imax-K_{imin}}} = \frac{K_i - 0}{1 - 0} \qquad 10(b)$$

$$K'_d = \frac{K_d - K_{dmin}}{K_{dmax-K_{dmin}}} = \frac{K_d - 0}{0.01 - 0} \qquad 10(c)$$

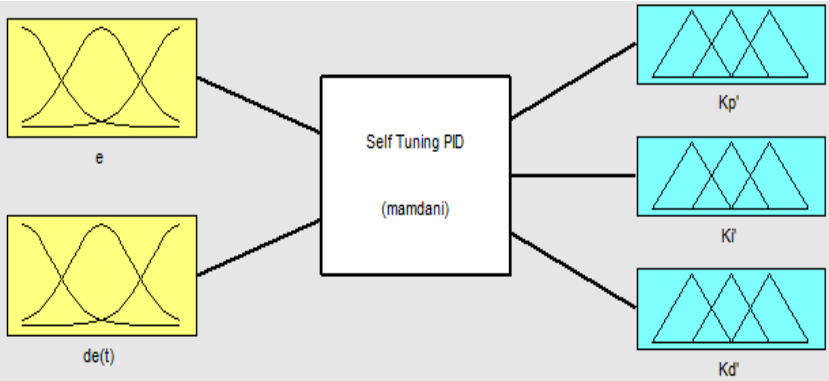

Figure 10. Fuzzy inference block

Hence the K'_p, $K'_i$and K'_d values can be got from equation. (10). The membership functions of these inputs fuzzy sets are shown in Figure 11 and 12. The linguistic variable levels are assigned as NB: negative big; NS: negative small; ZE: zero; PS: positive small; PB: positive big. These levels are chosen from the characteristics and specification of the SMA actuator. The ranges of these inputs are from -0.1 to 0.1, which are obtained from the absolute value of the system error and its derivative through the gains, whereas the membership functions of outputs K_p', K_i' and K_d' are shown in Figure.13. The linguistic levels of these outputs are assigned as S: small; MS: medium small; M: medium; MB: medium big; B: big, where the range varies from 0 to 1.

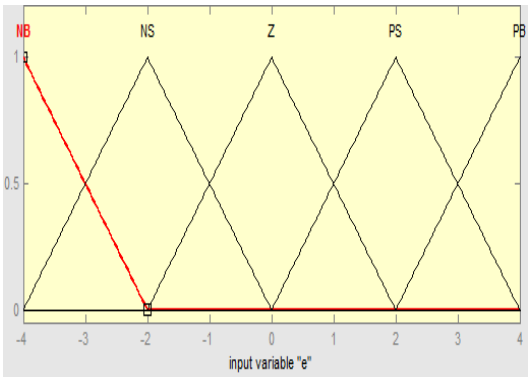

Figure 11. Membership function of *e*(*t*)

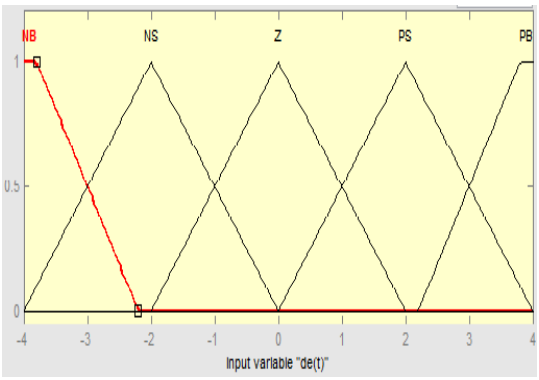

Figure 12. Membership function of *d e*(*t*)

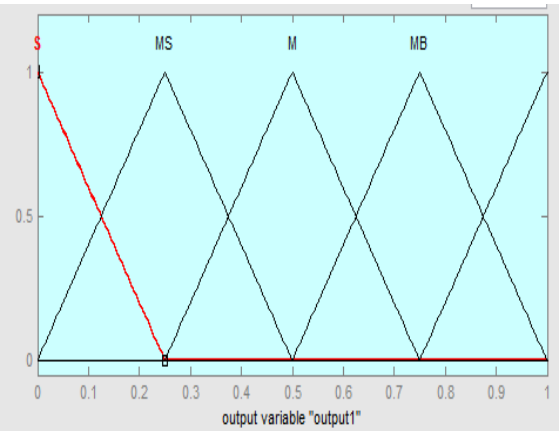

Figure 13. Membership functions of K_p', K_i' and K_d'

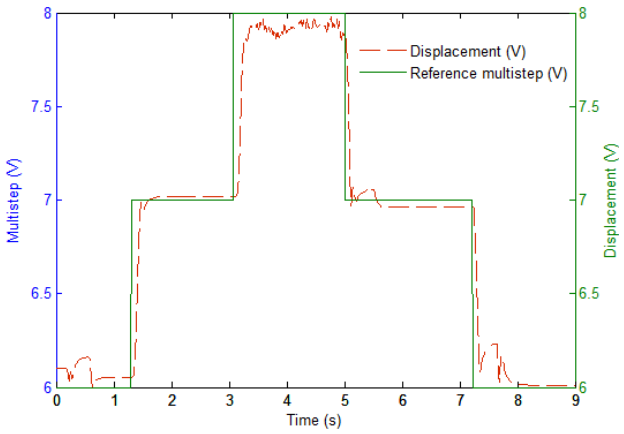

Figure 14. Multi step tracking

VI. EXPERIMENTAL AND SIMULATION RESULTS

Experiments were performed to examine the angular trajectory tracking of the robotic arm using the PID control technique. To protect the SMA actuators from overheating, the applied current was limited to 210 mA. The repetitive step tracking of the arm is shown in Figure 14. The strain of the SMA actuator changes when it tracks the input reference signal. This motion of the arm is monitored by laser displacement sensor (Aquity AR200).Figure 15(a) represents the tracking of a sinusoidal and square reference trajectory by the SMA actuators in closed loop with a frequency of 1Hz.The electrical resistance change in the SMA actuators and the current signal driving the actuators are shown in Figure15 (b) and 15(c) respectively. Figure 15(d) represents the differential torque acting on the manipulator. Subsequently the arm trajectory for a triangle wave with an input frequency of 1Hz is shown in Figure16.

VII. CONCLUSION

The paper presents the design, model and control of an antagonistically connected SMA wire actuator suitable for any robotic application. System identification technique is employed to obtain a state space model of the system. The self-tuning fuzzy PID controller employed here uses strain as a feedback signal and drives the actuators. The experimental results indicate that the controller can perform well in regulating the one joint arm manipulator to closely track the desired reference signal with a frequency of 1Hz, achieved smaller transient error and the appropriate selection of the pulley radius made the controller to track effectively and also retain stable behavior. The control scheme applied to the one joint arm driven by antagonistic

SMA actuator achieves more accurate and dynamic tracking performance compared to conventional controllers.

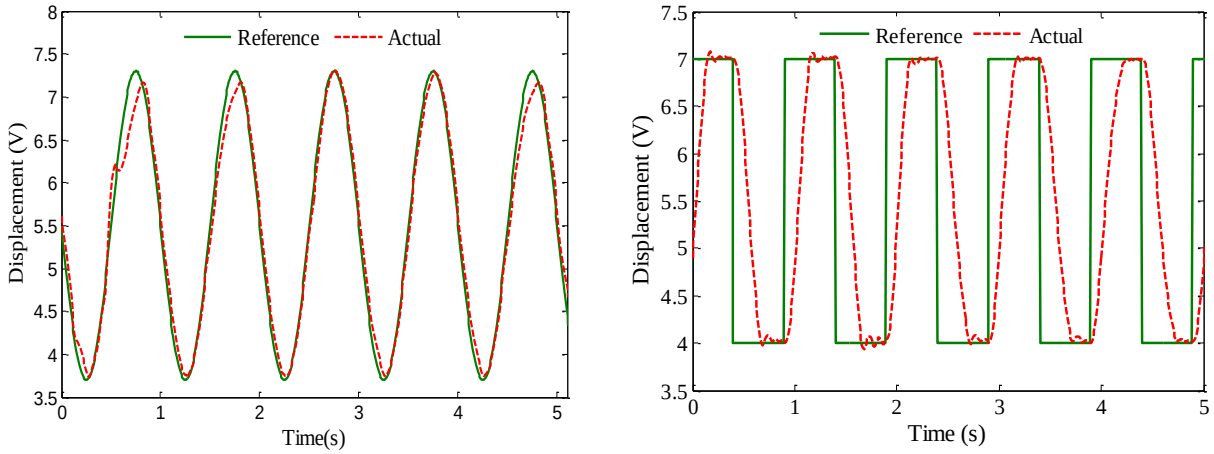

(a)

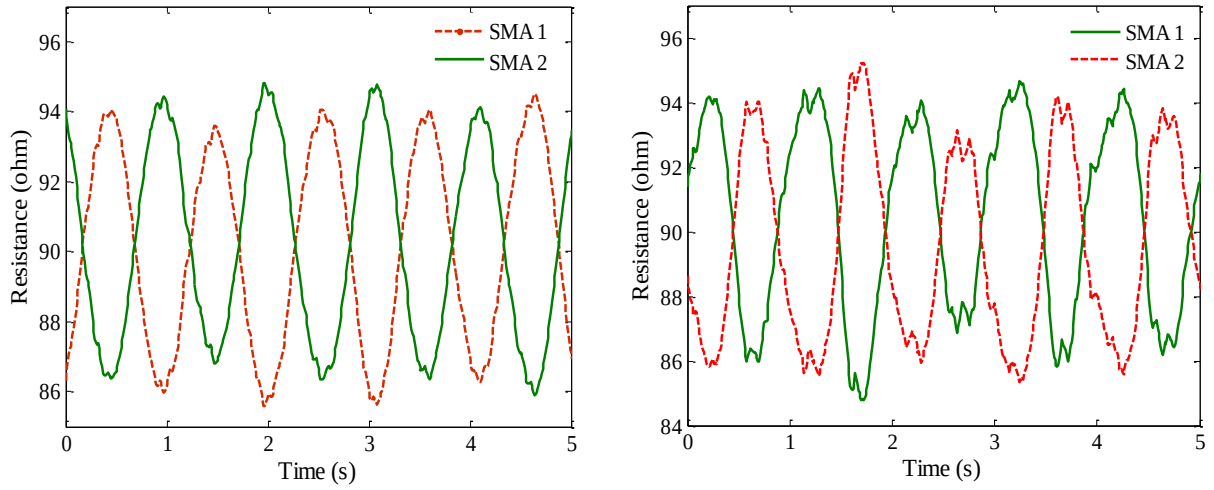

(b)

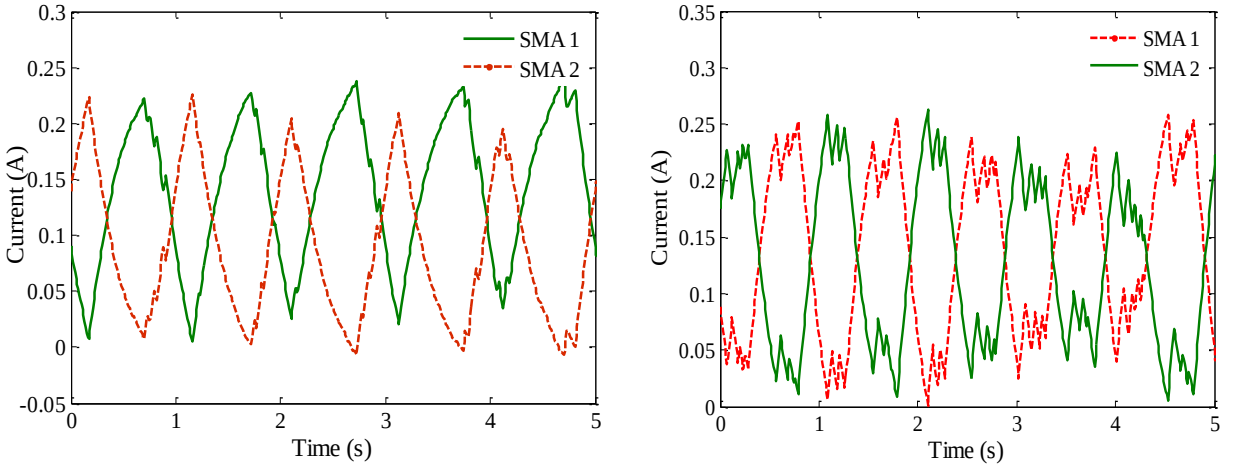

(c)

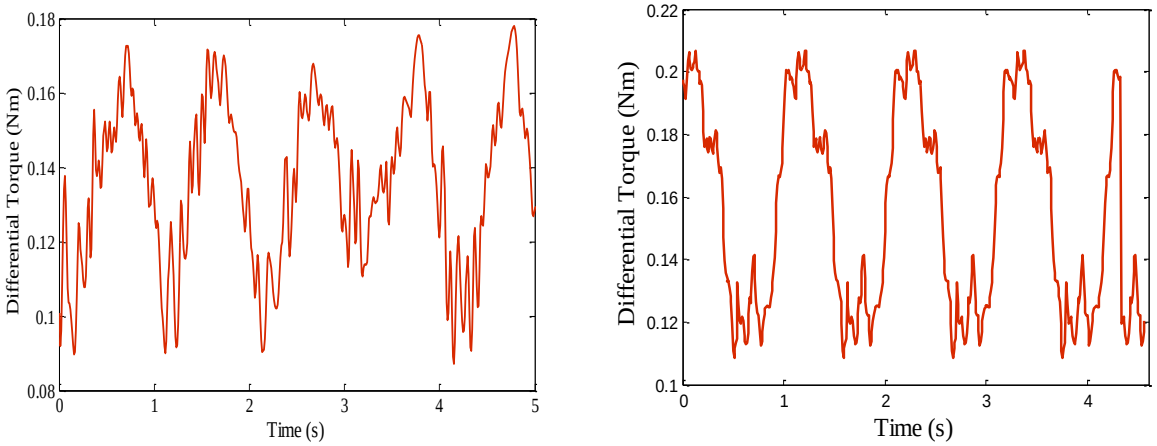

(d)

Figure 15. Experimental results for tracking a sinusoidal and square trajectory (a) desired and actual angular position (b) resistance change in SMA wire (c) current signal to the SMA wires (d) differential torque developed

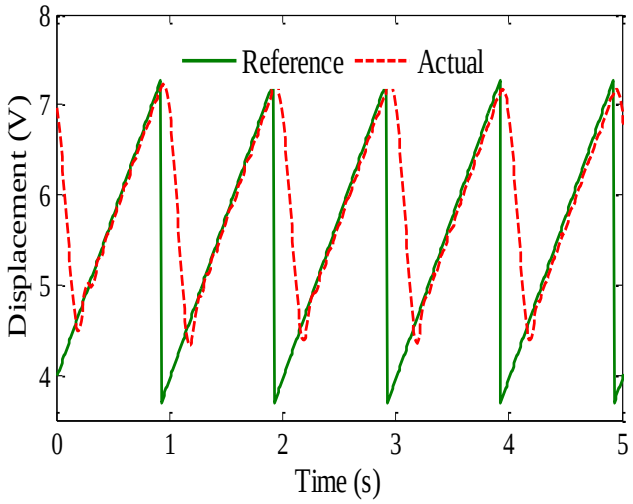

(a)

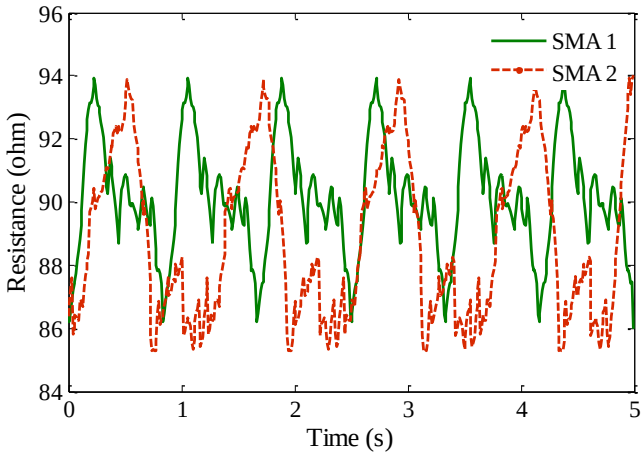

(b)

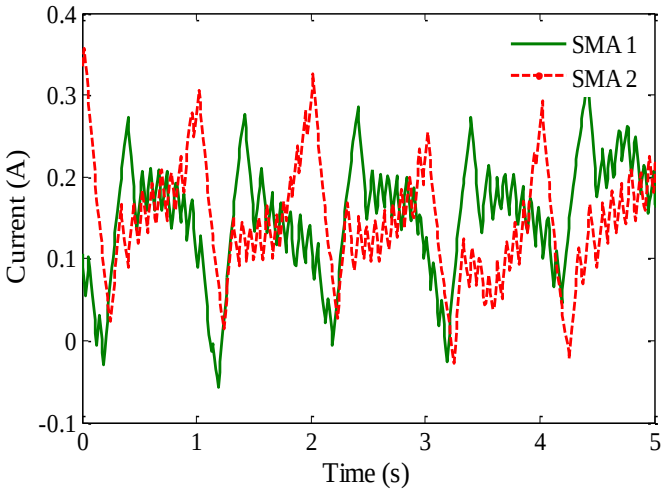

(c)

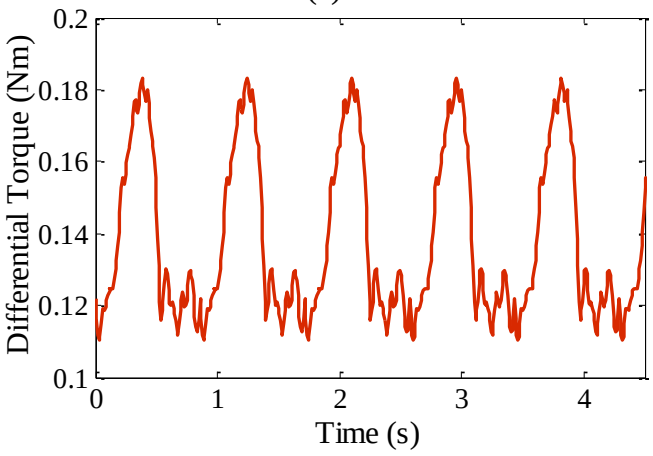

(d)

Figure 16. Experimental results for tracking a sinusoidal trajectory
(a) Desired and actual angular position (b) Resistance change in SMA wire
(c) Current signal to the SMA wires (d) Differential torque developed

REFERENCES

[1] K.F. Beyeler, A. Neild, S. Oberti, D. J. Bell, Y. Sun, J. Dual and B. J. Nelson, Monolithically Fabricated Microgripper with Integrated Force Sensor for Manipulating Microobjects and Biological Cells Aligned in an Ultrasonic Field, J. Microelectromech. Syst., Vol 16 No 1, pp. 7–15, 2007.

[2] T. C. Duc, G. K. Lau, J. F. Creemer and P. M. Sarro, ElectrothermalMicrogripper with Large Jaw Displacement and Integrated Force Sensors,J. Microelectromech. Syst., Vol 17 No6, pp. 1546–1555, 2008.

[3] S. Konishi, F. Kawai and P. Cusin, Thin Flexible End-effector using Pneumatic Balloon Actuator, Sens. Actuators A, 89, pp. 28-35, 2001.

[4] R. Lumia and M. Shahinpoor, IPMC Microgripper Research and Development, J. Phys.: Conf. Ser., 127, 012002, 2008.

[5] R. Pérez, J. Agnus, C. Clévy, A. Hubert, and N. Chaillet, Modeling, Fabrication, and Validation of a High-Performance 2-DoF Piezoactuator for Micromanipulation, IEEE/ASME Trans. Mechatron., 10(2), pp. 161-171, 2005.

[6] D.H. Kim, B. Kimand H. Kang, Development of a Piezoelectric Polymer-based Sensorized Microgripper for Microassembly and Micromanipulation, Microsystem Technologies, 10, pp. 275–280, 2004.

[7] Z. W. Zhong and C. K. Yeong, Development of a Gripper Using SMA Wire, Sens. Actuators A, 126(2), pp. 375–381, 2006.

[8] J. H. Kyung, B. G. Ko, Y. H. Ha, and G. J. Chung, Design of a Microgripper for Micromanipulation of Microcomponents Using SMA Wires and Flexible Hinges, Sens. Actuators A, 141, pp. 144–150, 2008 .

[9] J. M. Stevens and G. D. Buckner, Actuation and control strategies for miniature robotic surgical systems, ASME J. Dyn. Syst., Meas. Control, Vol. 127, pp. 537–549. 2010.

[10] F. Morra, R. Molfino and F. Cepolina, Miniature gripping device, Proc. Int. Conf. Intell. Manipulation Grasping, pp. 363–368. 2004.

[11] H. Fischer, B. Vogel and A.Welle, Application of shape memory alloy in medical instruments, Minimally Invasive Therapy Allied Technol., Vol. 13, No. 4, pp. 248–253, 2004.

[12] M. Hashimoto, M. Takeda, H. Sagawa, I. Chiba and K. Sat, Shape memory alloy and robotic actuators, J. Robot. Syst., Vol. 2, pp. 325, 1985.

[13] K. Dhanalakshmi, Aditya Avinash, M. Umapathy, M. Marimuthu, Experimental study on vibration control of shape memory alloy actuated flexible beam, International Journal on Smart Sensing and Intelligent Systems, Vol 3,No 2, pp. 156-175, 2010.

[14] Nakshatharan S, Ruth D J S, Dhanalakshmi K, Design based active vibration control of a flexible structure using shape memory alloy wire actuators, IEEE International Conference on Sensing Technology, pp. 476-480, Dec 2012.

[15] Ruth D J S, Nakshatharan S, Dhanalakshmi K, Angular trajectory tracking using antagonistic shape memory alloy actuators, IEEE International Conference on Sensing Technology, pp.748-753, Dec 2012.

[16] M. Moallem and J. Lu, Application of shape memory alloy actuator for flexure control: Theory and experiments, IEEE Trans. Mechatronics, 2005, Vol. 10, No. 5, pp. 495–501.

[17] N.Ma and G Song, Control of shape memory alloy actuator using pulse width modulation, Smart Mater. Struct., Vol.12, pp. 712–719. 2003.

[18] Kevin M. Lynch, Matthew T. Mason, Dynamic manipulation with a one joint robot, IEEE International Conference on Robotics and Automation, Vol 1,pp 359-366,1997.

[19] S. Majima, K. Kodamaand T. Hasegawa, Modelling of shape memory alloy actuator and tracking control system with the model, IEEE Transactions on Control System Technology, Vol 9, pp.54, 2001.

[20] K. Kwan Ahn and B. Kha Nguyen, Position Control of Shape Memory Alloy Actuators using Self-Tuning Fuzzy PID Controller, J. Control Automation, Vol. 4, pp. 756-762, 2006.

[21] V. A. Tabsizi and M. Moallem, Nonlinear Position Control of Antagonistic Shape Memory Alloy Actuators, Proceedings of American Control Conference, pp 88-93, 2007.

[22] H. Li, C. Mao and J. Ou, Strain self-sensing property and strain rate dependent constitutive model of austenitic shape memory alloy: Experiment and Theory, Journal of Materials in Civil Engineering,Vol.17, No 6,pp 676-685,2005.

[23] Zulfatman and M. F. Rahmat, Application of self-tuning Fuzzy PID Controller on Industrial Hydraulic Actuator using System Identification Approach, International Journal on Smart Sensing and Intelligent Systems, Vol. 2, No. 2,pp 246-261,June 2009.